

Research Article

Theme: Next Generation Formulation Design: Innovations in Material Selection and Functionality
Guest Editors: Otilia M. Koo, Panayiotis P. Constantinides, Lavinia M. Lewis, and Joseph Reo

Spray-Dried Thiolated Chitosan-Coated Sodium Alginate Multilayer Microparticles for Vaginal HIV Microbicide Delivery

Jianing Meng,¹ Vivek Agrahari,¹ Miezan J. Ezoulin,¹ Sudhaunshu S. Purohit,² Tao Zhang,¹ Agostino Molteni,³ Daniel Dim,³ Nathan A. Oyler,² and Bi-Botti C. Youan^{1,4}

Received 12 August 2016; accepted 12 October 2016; published online 30 January 2017

Abstract. It is hypothesized that novel thiolated chitosan-coated multilayer microparticles (MPs) with enhanced drug loading are more mucoadhesive than uncoated MPs and safe *in vivo* for vaginal delivery of topical anti-HIV microbicide. Formulation optimization is achieved through a custom experimental design and the alginate (AG) MPs cores are prepared using the spray drying method. The optimal MPs are then coated with the thiolated chitosan (TCS) using a layer-by-layer method. The morphological analysis, *in situ* drug payload, *in vitro* drug release profile, and mucoadhesion potential of the MPs are carried out using scanning electron microscopy, solid-state ³¹P NMR spectroscopy, UV spectroscopy, fluorescence imaging and periodic acid Schiff method, respectively. The cytotoxicity and preclinical safety of MPs are assessed on human vaginal (VK2/E6E7) and endocervical (End1/E6E7) epithelial cell lines and in female C57BL/6 mice, respectively. The results show that the MPs are successfully formulated with an average diameter ranging from 2 to 3 μm with a drug loading of 7–12% *w/w*. The drug release profile of these MPs primarily follows the Baker-Lonsdale and Korsmeyer-Peppas models. The MPs exhibit high mucoadhesion (20–50 folds) compared to native AGMPs. The multilayer MPs are noncytotoxic. Histological and immunochemical analysis of the mice genital tract shows neither signs of damage nor inflammatory cell infiltrate. These data highlight the potential use of TCS-coated AG-based multilayer MPs templates for the topical vaginal delivery of anti-HIV/AIDS microbicides.

KEY WORDS: microbicide; microparticles; mucoadhesive; spray drying; thiolated chitosan.

INTRODUCTION

An ideal vaginal drug delivery system should be easy to administer, not cause discomfort to improve patient compliance and have a reduced number of doses required to the treatment (1).

To meet these requirements, various vaginal drug carriers have been developed (2–5). However, in most of these formulations, the encapsulation of a water-soluble small molecular drug is a serious problem associated with drug % payload. Recently, a special attention has been focused on the development of spray-dried microparticles (MPs) as an alternative solution (6).

Spray drying is a rapid and simple process based on the solvent atomization and evaporation process. The atomized polymeric droplets containing the drug are transformed in solid particles by a stream of heated air (7). The spray drying method not only typically produces spherical MPs with a narrow size distribution but also enables the encapsulation of both hydrophilic and hydrophobic drugs with relatively high efficiency and yield (8,9).

The main advantages of MPs over traditional vaginal dosage forms such as gels, creams, rings, and films are as follows: the generation of a sustained drug release profile following the application of a single dose, a proper spreading over the vaginal epithelium, the protection of the drugs, and ability to reduce drug toxicity. To further prolong the residence time on the site of the treatment, a thiolated chitosan (TCS) is used to coat the MPs. TCS has been shown to possess high mucoadhesive properties due to

Jianing Meng and Vivek Agrahari contributed equally to this work.

Electronic supplementary material The online version of this article (doi:10.1208/s12248-016-0007-y) contains supplementary material, which is available to authorized users.

¹ Laboratory of Future Nanomedicines and Theoretical Chronopharmaceutics, Division of Pharmaceutical Sciences, University of Missouri-Kansas City, Kansas City, Missouri 64108, USA.

² Department of Chemistry, University of Missouri-Kansas City, Kansas City, Missouri 64110, USA.

³ School of Medicine, University of Missouri-Kansas City, Kansas City, Missouri 64108, USA.

⁴ To whom correspondence should be addressed. (e-mail: youanb@umkc.edu)

the thiol groups present on the chitosan backbone, which can form disulfide bonds with the thiol groups present on the mucus substructures (10).

In this study, a hydrophilic anti-HIV microbicide, tenofovir (TFV), is encapsulated within the spray-dried sodium alginate (AG)-based MPs. The MPs are coated with TCS based on the charge-charge interaction between AG and TCS. It is postulated that these MPs may prolong the drug retention time and controlled release profile and could be a potential vaginal drug delivery system with increased encapsulation efficiency of water-soluble small molecule drugs, such as TFV.

MATERIALS AND METHODS

Materials

Sodium alginates (AG) with low (viscosity ~500 cp, 5 % w/v in water) and high molecular weight, Mw (viscosity ~1000 cp, 5 % w/v in water) are provided by Spectrum Chemical (New Brunswick, NJ, USA). Chitosan with the Mw of 50–190 kDa, mucin, periodic acid, and Schiff reagent kit are purchased from Sigma Aldrich (St. Louis, MO, USA). Thiolated chitosan (TCS) is prepared in the lab as reported elsewhere (11). TFV is purchased from Zhongshuo Pharmaceutical Co. Ltd. (Beijing, China). Sodium triphosphate pentabasic (TPP) is supplied by Fisher Scientific (Pittsburgh, PA, USA). The CytoTox-ONE™ and CellTiter 96™ Aqueous kits are purchased from Promega (Madison, WI, USA).

Methods

Formulation of Spray-Dried MPs

To prepare TFV-loaded AGMPs, different amounts of AG and TFV (Table I) are dissolved in 40 ml of deionized water, and the ratio of AG to TFV is 5:1 (*w/w*). The solution is then spray dried using a Buchi Mini Spray Dryer, Model 290 (Buchi Laboratories - Technik AG, Flawil, Switzerland). Then, the formulated MPs are stored at 4°C for further analysis.

In order to optimize the preparation conditions, a custom design with 3 factors and 16 run is used to study the influence of the formulation variables on the yield. The independent variables, polymer (AG) molecular weight (Mw), polymer concentration, and inlet temperature (*T*), are represented by X_1 , X_2 , and X_3 , respectively. The percent yield, which is the dependent variable, is represented by *Y*. These variables and their coded factors are listed in Table I. All independent variables in this work are selected based on data from our preliminary experiments. The yield of the spray drying process is calculated using Eq. 1 below:

Table I. Independent and Dependent Variables and Their Levels in Custom Design

Variables		Value		
Independent	Polymer (AG) Mw (X_1)	Low	High	
	Polymer (AG) concentration (X_2)	5 mg/ml	10 mg/ml	15 mg/ml
	Inlet temperature (X_3)	100°C	125°C	150°C
Dependent	Yield (<i>Y</i>)			

$$\text{Yield}(\%) = \frac{\text{Total mass of MPs powder collected}}{\text{Total mass of initial ingredients in the formulation}} \times 100 \quad (1)$$

Preparation of the Multilayer MPs

The preparation of MPs layer by layer is adapted from the method of Li *et al.* (12). The multilayer MPs are obtained by alternately coating AG and TCS on the surface of the particles (Supplementary Fig. S1). Briefly, 40 mg of CaCl₂ and 2 mg of TCS are dissolved in 1 ml of acetic acid solution (pH 5). A total of 1 mg of spray-dried AGMPs are subsequently suspended into the above TCS solution. Then, the resulting suspension is stirred for 2 h. The product is collected by centrifugation at 10,000 rpm for 10 min (Beckman Coulter Inc., Pasadena, CA, USA) and washed once thoroughly with water. This first product is TCS-coated single layer MPs (SLMPs). To prepare the double layer MPs (DLMPs), AG and TCS are separately dissolved in 0.1% acetic acid solution (pH 5) at a concentration of 2 mg/ml, respectively. At this pH, both TCS (weak acid, pKa 6.5) and AG (weak base, pKa 4.2) mainly exist in ionized form in the two different solvents (13). Then, the SLMPs are suspended in 1 ml of AG solution, stirred, centrifuged, and washed as described above, followed by suspension in 1 ml of TCS solution for 10 min. The resulting DLMPs are collected by centrifugation. The triple layer MPs (TLMPs) could thus be obtained by repeating the above preparation steps of DLMPs. The percent drug loading is determined using ³¹P solid-state NMR as described in the Supplementary Material.

Surface Characteristics

The zeta potential of the MPs is determined using a zeta sizer (Zetasizer Nano ZS, Malvern Instruments Ltd, Worcestershire, UK). Measurements are made in triplicate (*n* = 3) at 25°C.

The surface chemistry is determined by a Nicolet™ 860 iS™10 FT-IR Thermo Electron spectrometer (Thermo Scientific, West Palm Beach, FL, USA). Before analyzing each sample, the background spectrum is collected at ambient conditions. The MPs are then scanned over the wavenumber range of 650 and 4000 cm⁻¹. The FT-IR spectra are recorded by OMNIC V 7.0 spectra software.

The morphology of the MPs is analyzed by scanning electron microscopy (SEM). A small amount of the MPs powder is mounted on 1/2-in. aluminum stubs with double-sticky carbon tape and sputter coated (Emitech EMS575SX) with approximately 20 nm thickness of gold-palladium alloy. The sample is then visualized under a FEI/Philips XL30 Field-Emission Environmental SEM (Philips/FEI, Eindhoven, Netherlands) at 5 kV. Digital images are acquired with ORIUS™ SC 100 large format (II Megapixel) CCD camera (Gatan, Pleasanton, CA, USA). The diameter of the MPs in the SEM images is estimated based on a count of at least 100 particles using Image Pro Plus software (Image Pro Plus 6.0, Media Cybernetics, Silver Spring, MD, USA).

In Vitro Drug Release Profile

The *in vitro* release of TFV from different MPs is evaluated using the dialysis method (14). Briefly, one milligram/ml of MP suspension is prepared in vaginal fluid simulant (VFS) or semen fluid simulant (SFS) media, according to previous reports (15,16). This suspension is then placed in Spectra/Por cellulose ester membrane dialysis bag (Spectrum Laboratories Inc. Rancho Dominguez, CA, USA) with 10–12 kDa Mw cutoff and immersed into 20 ml of the same media at 37°C in a thermostatically controlled shaking water bath (BS-06, Lab Companion, Seoul, South Korea). At predetermined time intervals, the whole media is removed and replaced by fresh media. The concentration of the drug in the media is determined by a GENESYS 10 Bio UV-Visible Spectrophotometer (Thermo Scientific, Waltham, MA, USA) at 259 nm. Each experiment is run in triplicate together with a blank (control). In order to find out the mechanism of drug release from the formulations, the data distributions are fitted to various kinetics models (first-order, Higuchi, Baker-Lonsdale, and Korsmeyer-Peppas model), using Microsoft Excel add-in DDSolver software (17). The equation and parameters of these models are shown in Supplementary Table S3.

Mucoadhesion Study

To assess the amount of mucin adsorbed by the MPs, a periodic acid/Schiff (PAS) colorimetric method is used (18). Briefly, mucin is dissolved in VFS and SFS and the MPs powder is suspended in the same solution at the mucin/MPs ratio of 0.1, 1, and 2. The suspension is maintained in the above shaking water bath at 37°C for 30 min with an agitation speed of 100 rpm and then centrifuged at 4,000 rpm for 2 min. The supernatant is removed, 0.2 ml of periodic acid reagent is added and incubated at 37°C for 2 h, followed by the addition of 0.2 ml Schiff reagent and incubation at room temperature for 30 min. The absorbance of the solution is recorded at 555 nm by the above UV spectrophotometer. The mucin content is calculated from the standard calibration curve. The sprayed AGMPs and mucin solution without MPs are used as controls. Each experiment is performed in triplicate. The mucin adsorption is estimated using Eq. 2:

$$\text{Mucin adsorption(\%)} = \frac{\text{Total mass of mucin-free mucin}}{\text{Total mass of mucin}} \times 100 \quad (2)$$

Cytotoxicity Studies

To perform the cytotoxicity studies, VK2/E6E7 (human vaginal keratinocyte) and End1/E6E7 (human endocervical epithelial) cell lines are grown in Keratinocytes-SFM medium supplemented with 1% penicillin/streptomycin and 10% (v/v) fetal bovine serum (FBS). Cells are seeded in 96-well plates at 37°C and humidified 5% CO₂ atmosphere till 80% confluence is achieved. Then, the original cell culture media is removed and substituted with media containing AGMPs, SLMPs, DLMPs, and TLMPs with different concentrations. Media with no MPs and 1% Triton-X 100 are used as negative and positive control samples, respectively. The well plates are then incubated at 37°C for 24 and 48 h (5).

In order to perform the lactate dehydrogenase (LDH) assay, the plates are equilibrated at room temperature for 10 min. One hundred microliters of CytoTox-ONE™ Reagent is added in each

well, followed by 30 s shaking and 10 min incubation at 37°C. Finally, 50 µl of stop solution is added. The fluorescence intensity is determined by a microplate reader at λ_{ex} 560 nm and λ_{em} 590. The percent LDH release is computed using the reagent manufacturer's protocol.

For cell viability determination, after the incubation time, the media in the wells is removed and substituted with fresh media. Twenty microliters of CellTiter 96® AQueous One Solution Reagent (Promega, Madison, WI, USA) is added to each well and incubated at 37°C for 4 h. The absorbance is recorded at a wavelength of 490 nm. The percent cell viability is computed using the reagent manufacturer's protocol.

In Vivo Safety Studies

Female C57/BL6 mice (8–12 weeks old) with an average body weight of 20 g are ordered from Jackson Laboratories (Harbor, ME). All animals are housed in the Laboratory Animal Resource Center (LARC) facility in the University of Missouri-Kansas City (UMKC) according to the Association for Assessment and Accreditation of Laboratory Animal Care (AAALAC) guidelines. The animal protocols used in this study are approved by UMKC Institutional Animal Care and Use Committee (IACUC). Mice are treated with 2 mg of subcutaneous medroxyprogesterone acetate (Greenstone, Peapack, NJ, USA) diluted in lactated Ringer's saline solution 4–5 days before the treatment to induce and maintain a diestrus-like state.

The DLMPs are suspended in PBS and a MPs dose of 475 mg/kg (in 30 microliters) is administered intravaginally to each animal and PBS are used as positive and negative controls, respectively. Once-daily administration is carried out using a flexible feeding needle (Cadence, Inc. Staunton, VA, USA). After completion of the 1- and 7-day intravaginal application, mice are euthanized by carbon dioxide (CO₂) asphyxiation. Their cervico-vaginal tissues are harvested. The collected tissues are formalin fixed and embedded in paraffin, cut into 5-mm sections, and stained as described below.

For hemotoxylin and eosin (H&E) staining, sections are deparaffinized in xylene and then passed through several changes of alcohol and then rinsed thoroughly with deionized water to rehydrate them. Hematoxylin is applied on the sections followed by eosin, and overstaining is removed by rinsing water. Thereafter, nuclei are stained blue, whereas the cytoplasm and extracellular matrix are stained pink (19). Images are captured using a Nikon Labophot-2 microscope (Nikon Instruments, Inc., Melville, NY) equipped with a PAXCam digital microscope camera and analyzed using PAX-it image management and analysis software (Midwest Information Systems, Inc., Villa Park, IL).

In order to identify eventually the inflammatory cell (CD45) infiltrations, genital tissue sections are analyzed after immunohistochemical (IHC) staining. Briefly, the sections are deparaffinized and rehydrated as described above. Antigen retrieval is performed using the steam heat method in citrate buffer/0.05% Tween-20 for 20 min. The tissue sections are then rinsed with Tris buffered saline/0.05% Tween-20 three times, followed by treatment with 3% v/v hydrogen peroxide in PBS for 10 min and blockage with 10% normal goat serum for 2 h (Vector Laboratories, Burlingame, CA). The solution of anti-CD45 used as a primary antibody from Santa Cruz Biotechnology, Inc. (Dallas, TX) is diluted in 1.5% normal goat serum to 5 µg/ml (1:50) and applied to the tissue

Table II. Checkpoint Experiments Comparing Measured and Predicted Responses ($n = 3$)

Run no.	X_1	X_2 (mg/ml)	X_3 ($^{\circ}\text{C}$)	Measured Y (%)	Predicted Y (%)	Error%	t value	P value
C1	Low	7.5	113	53.2 ± 4.8	51.3	4.2	0.41	0.72
C2	High	12.5	138	37.7 ± 7.5	32.7	15.4	0.66	0.58
C3	Low	6.1	142	62.6 ± 6.7	59.0	6.2	0.55	0.64

changed simultaneously. The main effect of all independent variables and their interactions on the dependent variable (yield) is shown in Fig. 1a, and the values on the x-axis of the Pareto charts represent the standardized effects. The factors whose length passed the blue vertical line ($t_{\text{critical}} = 2.36$ at $P < 0.05$) are identified as statistically significant (21). Figure 1b is a desirability and prediction plot showing the effect of the independent variables on the yield. The solid black line and the dashed boundary lines represent the predicted values of the yield with their 95% confidence data distribution limit, respectively. In order to maximize the yield, the optimum condition is selected through the mathematical optimization process: low MW AG concentration of 6.13 mg/ml, and inlet T 142 $^{\circ}\text{C}$.

The relationship between the actual values and the theoretical values of the yield is investigated by a check point analysis. The measured and predicted values of the yield at three selected points (two random points and the optimal point) are shown in Table II. The differences of all the points appear to be statistically insignificant, indicating that this model is valid for predicting the yield.

Characterization of the MPs

The nature of the main ingredients on the MP surface after the coating process can be estimated from the zeta potential measurement (Fig. 2a). A reversal in the surface

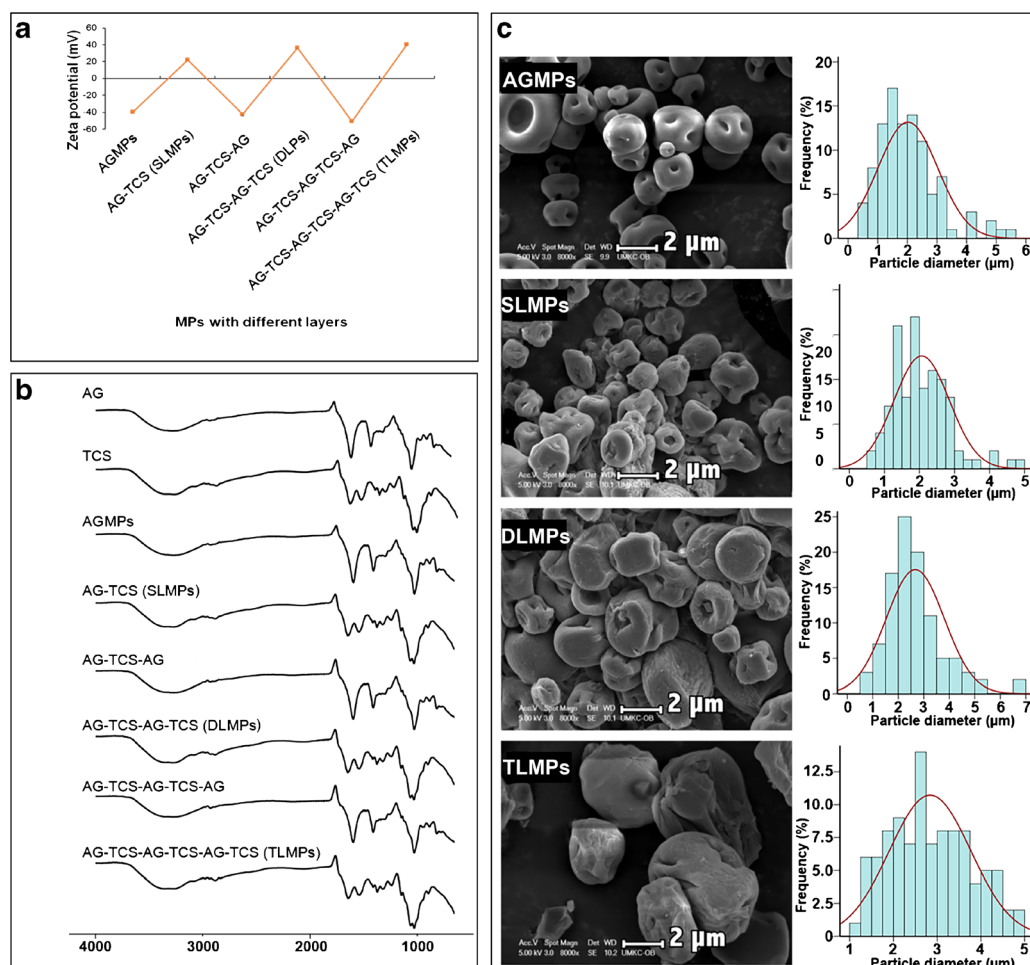


Fig. 2. Surface analysis of the microparticles (MPs). **a** Change in zeta potential values of the alginate microparticles (AGMPs) coating with positively charged thiolated chitosan (TCS) and negatively charged alginate (AG) ($n = 3$). **b** Change in FT-IR of AGMPs coating with TCS and AG. **c** SEM image (left) and size distribution (right) of single layer microparticles (SLMPs), double layer microparticles (DLMPs), and triple layer microparticles (TLMPs)

Table III. Physical and Chemical Properties in the Multilayer MPs (n =)

Formulation	First TCS layer	Second TCS layer	Third TCS layer	Drug loading (%w/w)	Zeta potential (mV)	Mean diameter (μm)
SLMPs	+	–	–	17.8 ± 0.3	2.1 ± 0.8	25.2 ± 1.0
DLMPs	+	+	–	12.3 ± 0.2	2.7 ± 1.1	33.4 ± 0.5
TLMPs	+	+	+	7.2 ± 0.2	2.8 ± 1.0	35.5 ± 0.4

charge of the MPs is expected as oppositely charged polymers are adsorbed onto their surface. The zeta potential of native AG and TCS is found to be -42.0 ± 1.5 and $+35.5 \pm 1.5$ mV ($n=3$) (22). The coating by these different layers is further confirmed by FT-IR spectroscopy (Fig. 2b). Both native AG and native TCS exhibit a broad absorption peak at around 3100 to 3650 cm^{-1} and weak absorption peaks at 2890 cm^{-1} , attributed to their hydrogen bond stretching vibration and the CH stretch, respectively. TCS shows two characteristic peaks at 1520 and 1650 cm^{-1} , due to the amide (CO-NH-) and the amine (-NH₂) absorption band, respectively. The native AG reveals two sharp and characteristic peaks at 1610 and 1415 cm^{-1} assigned to the carboxylic acids (COO⁻).

Table III describes the TFV encapsulation, zeta potential, and mean diameter of the MPs with different layers. The percent drug loading slightly decreases due to two factors: (i) the presence of additional layers that increase the total mass of polymer and (ii) the increased drug loss during additional

washings. Layer-by-layer deposition also results in a slight increase in the particle size as shown in Fig. 2c.

In Vitro Drug Release Profile of the MPs

The drug release profile of the MPs in both VFS and SFS (Fig. 3) is characterized as a short-lasting burst release followed by a longer lasting sustained release. The spray-dried AGMPs alone are used as a control, in which, a burst release is observed, as AG is entirely solubilized without calcium chloride and TCS. After TCS coating, the drug release rate is reduced due to the addition of layers. As the number of layers is increased, so does the drug diffusion pathlength from the interior to the outer surface region of the MPs, therefore decreasing the release rate. Moreover, increasing the particle size leads to reduced specific surface area for larger MPs, which also contributes to the lower drug release rate (23).

To elucidate the drug release mechanism of the core-shell MPs, their drug release profiles are fitted to a series of known release kinetic models. The first-order release model represents the system where the drug release rate is concentration dependent and governed by the drug intrinsic properties. The Higuchi model is developed to describe the release of water-soluble (or low-soluble) drugs incorporated in solid (or semi-solid) matrixes. The Baker-Lonsdale model characterizes the controlled drug release from a spherical matrix. This model is generally applied to analyze the release of nano- and microparticles. The Korsmeyer-Peppas model is a semi-empirical model, in which the n value is used to study different mechanisms of the drug payload release (24). The results of the release data modeling are summarized in Table IV, and the quality of each model is determined using correlation coefficient (r^2) and Akaike information criterion (AIC) (25). In VFS, the drug release from SLMPs follows mostly the first-order kinetic, while the drug release from DLMPs and TLMPs is governed by the Baker-Lonsdale model. In SFS, the release of TLMPs fits the same model as in VFS, while the release profile of SL and DLMPs can be better described by the Korsmeyer-Peppas model, and the Korsmeyer-Peppas release exponent (n) is less than 0.5, indicating that diffusion is the controlling factor for drug release. According to the release modeling data, the release of drug form DLMPs and TLMPs would reach 95% after 173 and 346 h in VFS and 144 and 346 h in SFS, respectively.

Mucoadhesion of the MPs

To confirm the mucoadhesion of the TCS-coated MPs, their mucin adsorption is compared with that of the nonmucoadhesive MPs (AGMPs) using t test, which is a

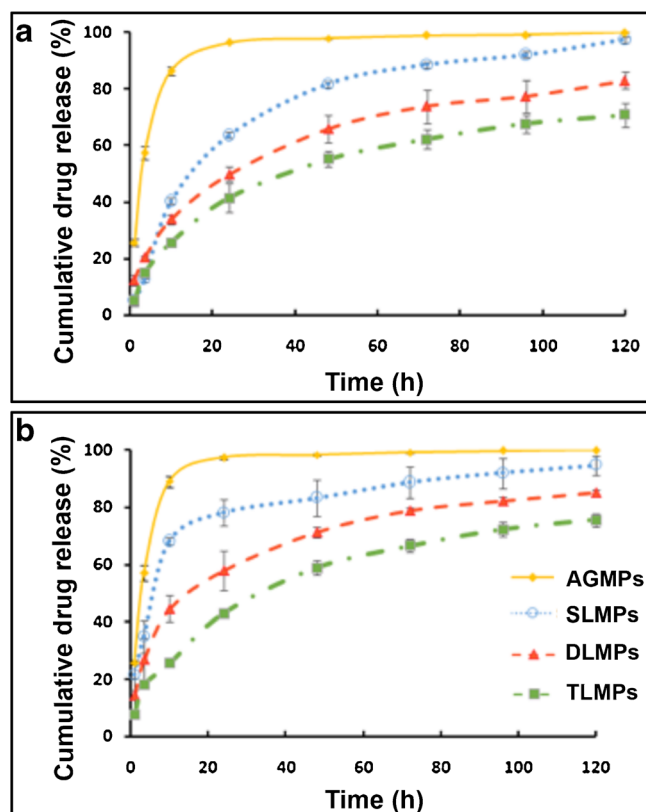


Fig. 3. In vitro release profile of drug from alginate microparticles (AGMPs), single layer microparticles (SLMPs), double layer microparticles (DLMPs), and triple layer microparticles (TLMPs) in vaginal fluid simulant (a) and semen fluid simulant (b) ($n=3$)

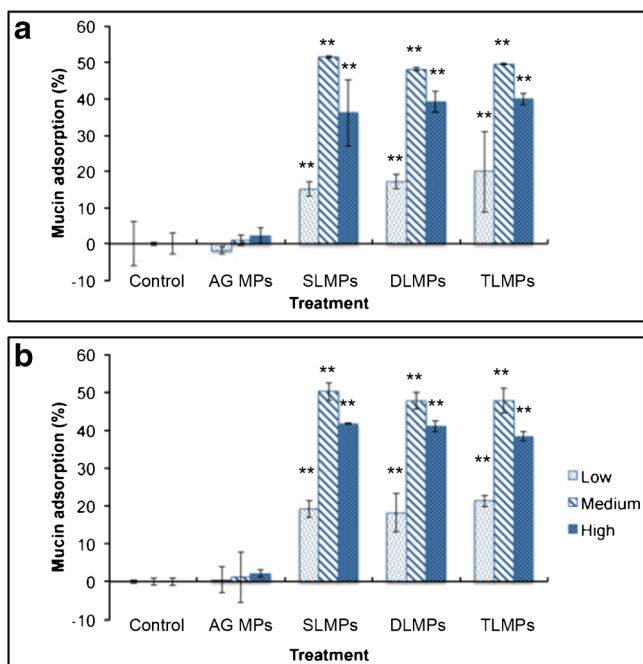


Fig. 4. Mucin adsorption of alginate microparticles (AGMPs), single layer microparticles (SLMPs), double layer microparticles (DLMPs), and triple layer microparticles (TLMPs) in VFS (a) and SFS (b), ($n = 3$). * $P < 0.05$ vs. AGMPs, ** $P < 0.01$ vs. AGMPs

commonly used statistic method to determine if the averages of two sets of data are significantly different from each other. As shown in Fig. 4, the P values of SLMPs, DLMPs, and TLMPs are less than 0.01 in both VFS and SFS, indicating very significant differences. The mucin adsorption of the TCS-coated MPs is increased by 10–20-fold compared to that of the nonmucoadhesive MPs whether group means differ from one another. In both VFS and SFS, the mucin adsorption is quite low, around 20%, when the mucin concentration is relatively low (0.1 mg/ml). When the mucin and MPs have the same concentration (1 mg/ml), the mucin adsorption increases to approximately 50%. Beyond a mucin concentration of 2 mg/ml, the percentage of mucin adsorption decreases to about 40% compared to that of the 1 mg/ml solution.

Cytotoxicity Study

According to Fig. 5a–d, compared to the LDH release of the negative control (media) treated cells, only the P values

of the positive control (Triton X-100) groups are less than 0.05. However, the null hypothesis is accepted for the MPs treatments: there is no statistical difference between the level of LDH release in media alone vs. that from MP treatment ($P > 0.05$), which indicated no impact of the MPs on the structural integrity of both cell lines. Similar results are observed in the cellular viability test. No significant reduction ($P > 0.05$) of cellular viability is found in the TFV-loaded MP-treated cells in comparison with that of the cells treated with media (Fig. 5e–g). These results suggest that the TFV-loaded MPs are not toxic to both vaginal (VK2/E6E7) and endocervical (End1/E6E7) epithelial cell lines at the concentration of 1 mg/ml up to 48 h.

In Vivo Safety Studies

DLMPs exhibiting medium drug loading (12.27% w/w) and release rate, are applied intravaginally to female C57/BL6 mice, and the optical micrographs of their genital tissues are examined. A representative H&E-stained vaginal tissue section is presented in Fig. 6a. Daily intravaginal exposure to the DLMPs does not lead to significant histological abnormalities. As a comparison, severe histopathologic changes, including ulceration and denudation (red arrows), are evident among mice treated with the positive control (4% N-9) for 24 h. The substantive difference of the vaginal epithelium integrity is found to be insignificant due to the recovery of the vaginal epithelium after 24 h postapplication (20).

The increase of CD45 lymphocytes indicates infiltration within the vagina epithelium, which is associated with increased susceptibility to HIV infection by facilitating the local viral expansion (26). After 4% N-9 application for 24 h and 7 days, compared to the PBS-treated tissue (negative control), the level of CD45-positive cells distributed within the N-9-treated vaginal epithelium is slightly elevated; however, the distribution of immune cells within the DLMP-treated vaginal tissue is similar to that of the negative control. The CD45-positive cells are identified by arrowhead marks in Fig. 6b. Collectively, the results indicate that there is no considerable infiltration by immune cells in the vaginal epithelium after DLMPs exposure for 24 h and 7 days.

DISCUSSION

The data shows that decreasing the polymer's concentration and Mw and increasing the mini spray dryer inlet T

Table IV. Mathematical Modeling for Drug Release from Different MPs in VFS and SFS

Media	MPs	First-order			Higuchi			Baker-Lonsdale			Korsmeyer-Peppas			
		k_1	r^2	AIC	k_H	r^2	AIC	k_B	r^2	AIC	k_{KP}	n	r^2	AIC
VFS (pH 4.2)	SL	0.040	0.985	41.6	10.04	0.926	54.3	0.003	0.970	47.0	14.9	0.41	0.947	53.6
	DL	0.022	0.846	55.4	8.43	0.934	48.6	0.002	0.991	32.8	14.8	0.37	0.989	36.3
	TL	0.014	0.859	53.5	7.13	0.965	42.3	0.001	0.990	32.5	10.2	0.42	0.982	38.9
SFS (pH 7.2)	SL	0.110	0.847	55.6	10.60	0.439	66.0	0.004	0.819	56.9	32.3	0.24	0.907	53.5
	DL	0.032	0.756	58.8	9.06	0.821	56.4	0.003	0.955	45.3	20.4	0.31	0.978	41.7
	TL	0.017	0.881	53.0	7.60	0.968	42.4	0.001	0.993	30.0	11.0	0.41	0.987	37.4

k_1 , k_H , k_{BL} , and k_{KP} represent the release rate constant of different model, and n is the release exponent

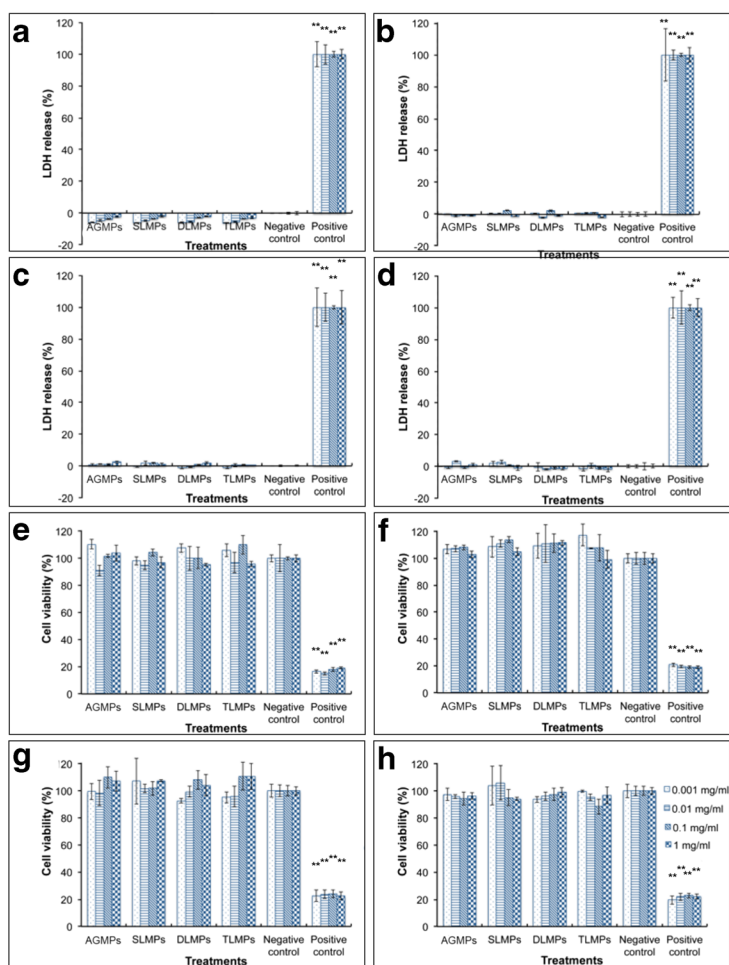


Fig. 5. Cytotoxicity study of alginate microparticles (AGMPs), single layer microparticles (SLMPs), double layer microparticles (DLMPs), and triple layer microparticles (TLMPs): Percent LDH release for VK2/E6E7 cell line after 24 h (a) and 48 h (b), Percent LDH release for End1/E6E7 cell line after 24 h (c) and 48 h (d), Percent viability for VK2/E6E7 cell line after 24 h (e) and 48 h (f), Percent viability for End1/E6E7 cell line after 24 h (g) and 48 h (h) ($n = 3$). * $P < 0.05$ vs. media, ** $P < 0.01$ vs. media

can significantly improve the process yield. The physical explanations of these observations are discussed in the three steps below.

Firstly, to obtain well-dispersed MPs, the concentration of the initial polymeric solution has to obey some conditions: (1) to generate particles with a relatively high density and good mechanical properties, the concentration of the polymer should be sufficiently high. (2) To allow its homogenous atomization, the viscosity of the solution should be relatively low, which consequently leads to a relatively low concentration, as the concentration is proportional to the viscosity at a given temperature (7). AG solution at a concentration lower than 5% (w/v) results in the formation of droplets and no dried powders based on preliminary experiments. At constant temperature and flow rate, more water needs to be removed with low solid content and high proportion of water, which leads to incomplete evaporation. Therefore, to efficiently and smoothly run the spray drying process, 5% (w/v) AG concentration is selected as the lowest limit of the polymer concentration. On the other hand, increasing polymer concentration results in increased solution viscosity. The solution viscosity is directly

proportional to the degree of atomization, which largely determines the efficiency of the spray drying process.

The mechanism of the atomization in spray drying is based on the immediate disintegration of liquid. At the nozzle orifice, the contact of the liquid with the high velocity gaseous medium creates high frictional force over the liquid surface. The liquid is broken up by the kinetic energy and is dispersed into smaller droplets. The entire process is the result of turbulence in the issuing liquid and the action of air force. However, it is opposed by the viscosity of the solution. As the feed solution's viscosity increases, more kinetic energy is used to overcome larger viscous force. This can be explained using the Reynolds (Re) number shown in Eq. 4:

$$Re = \frac{\rho wd}{\eta} \quad (4)$$

Where, ρ is the density of the liquid, w is the fluid velocity of the liquid, d is the inner nozzle diameter, and η is the viscosity (27).

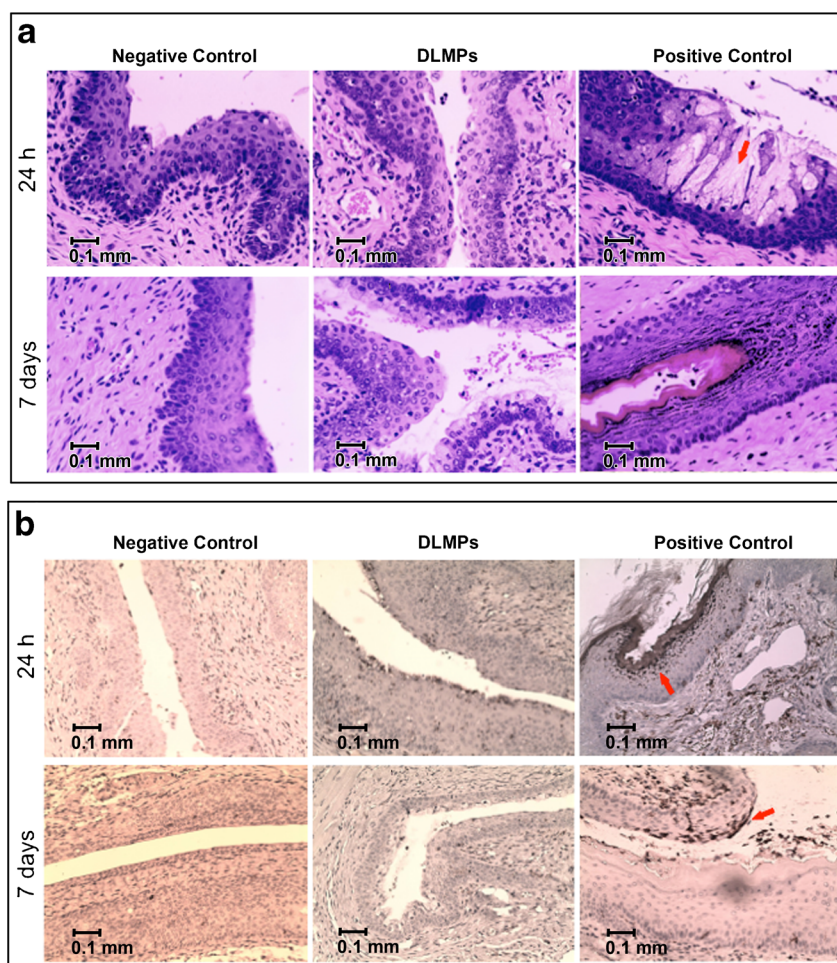


Fig. 6. *In vivo* safety evaluations in C57BL/6 mice vaginal tissue. **a** H&E stain of vaginal tissue after 24 h (top row) and 7 days (bottom row) exposure with PBS (negative control), double layer microparticles (DLMPs), and N-9 (positive control). **b** Immunohistochemical stain of vaginal tissues after 24 h (top row) and 7 days (bottom row) exposure with PBS, DLMPs, and N-9. Scale bar = 0.1 mm

An increase in solution viscosity lowers the Re and makes turbulence generation more difficult. Therefore, less energy of atomization is available for breaking up the droplets. The insufficient turbulence and energy transfer cause a wide droplet-size distribution throughout the resulting spray, and even a high percentage of liquid remains in the center of the spray as a solid jet. These large particles or jet cannot be completely dried before they deposit on the drying chamber wall (28). Therefore, when viscosity of the spraying solution is high, these semi-wet particles build up to form a wet deposit or even break off as wet lumps and stream down the wall. This is a well-known phenomenon that results in a reduced powder yield (29).

Secondly, the influence of Mw on the viscosity is shown in the Mark-Houwink equation as follows (30):

$$[\eta] = KMw^a \quad (5)$$

Where K and a are constants (Mark-Houwink constant).

The lowest molecular weight polymer (AG) leads to lower viscosity and higher Re , which allows sufficient turbulence in the polymeric solution during the spraying process, and hence resulting in higher yield.

Thirdly, by increasing the spray dryer inlet T (optimum = 142°C), the overall thermal efficiency is increased, leading to more effective drying and higher yield. The effect of the inlet T on spray drying process is shown as Eq. 6 (31,32):

$$\eta_{\text{overall}} = \frac{T_1 - T_2}{T_1 - T_0} \times 100 \quad (6)$$

Where η_{overall} denotes the overall thermal efficiency, T_1 is the inlet temperature, T_2 is the outlet temperature, and T_0 is the ambient temperature.

Besides the above three parameters, the feed flow rate of the spray drier also influences the final yield. Our preliminary experiments (data not shown) indicate that low flow rate favors the yield. This observation is consistent with the result of previous studies (33,34). Meanwhile, increasing the feed flow rate can easily cause droplets or wet stream instead of dried powder, especially when a solution with a high viscosity is used. Therefore, in this study, the feed flow rate is fixed at 0.35 ml/min, which is the lowest flow rate that the minispray dryer could achieve.

For the layer-by-layer method, the calcium ions are added as they can interact with the glucuronic sequences of AG *via* charge-charge interaction, and each calcium ion can be attached to two of the AG strands to form a matrix texture (35). Then, TCS is deposited on the surface of the MPs to generate a core-shell structure. However, TFV can easily diffuse out of the MPs across the single layer of the TCS shell. In order to further reduce the drug release rate, the second and third layers of TCS are applied as previously described.

The effective molar EC₅₀ of TFV is 5.0 to 7.6 μM (36). Based on the computed drug loadings, this concentration can be achieved when approximately 3.71, 2.58, and 1.52% of drug is released from the SLMPs, DLMPs, and TLMPs in the release media, respectively. According to the release pattern in Fig. 3, SLMPs, DLMPs, and TLMPs can provide effective TFV concentrate to exhibit an anti-HIV activity within 1 min after contact with both release media (VFS and SFS).

The mucus, which is secreted by the epithelium of the cervix, plays an important role in female reproductive function by facilitating the migration of the sperm toward the uterus (37). Mucus also provides a protective covering for the vaginal epithelium. It can be present as a luminal soluble, suspended form, or gel layer adherent to the mucosal surface (38). Mucin glycoprotein is the major component of mucus gels. In this study, the mucoadhesion of the MPs is assessed through the adsorption of mucin by MPs. It is reported that mucus compositional differences exist among individuals (39). Even for the same person, the amount of mucin in the female reproductive tract changes during the menstrual cycle. Prior studies suggest that in healthy women, the daily production of cervix mucus is around 20–60 mg/day. During the midcycle, it increases up to 700 mg/day and becomes less viscous in order to facilitate sperm migration (40). Therefore, different concentrations of mucin, low (0.1 mg/ml), medium (1 mg/ml), and high (2 mg/ml), are tested. In both VFS and SFS, the mucin adsorption is quite low, when the media mucin concentration is relatively low (0.1 mg/ml).

The possible reason is that both vaginal fluid and semen fluid contain soluble proteins, which are substituted by BSA in VFS and SFS. This negatively charged protein (zeta potential approximately equal to -25 mV) can interact with positively charged MPs by charge-charge interaction (41), therefore competing with the mucin adsorption process on the MPs surface. With relatively lower mucin concentration, individual MP has lower probability of interaction with mucin molecules, resulting in low mucin adsorption.

CONCLUSION

In this study, a custom experimental design is used to optimize the effect of formulation and process parameters of a spray-dried AGMPs (polymer Mw, polymer concentration, and inlet *T*, respectively) on the yield. The master AG core MPs is obtained when 6.13 mg/mL of the low-Mw AG is spray-dried at the inlet temperature of 142 °C. Based on the optimized MPs formulation, thiolated chitosan-coated multilayer MPs are prepared utilizing a layer-by-layer technique. These microspheres exhibit a high mucoadhesion (20–50 fold) property in both vaginal fluid and semen fluid simulants and are noncytotoxic to vaginal endocervical epithelial cells. The coated MPs are also safe *in vivo* based on H&E and IHC staining.

These data suggest that these MPs could potentially be a safe formulation for intravaginal delivery of anti-HIV microbicides.

ACKNOWLEDGMENTS

The work presented was supported by Award Number R01AI087304 from the National Institute of Allergy and Infectious Diseases. The content is solely the responsibility of the authors and does not necessarily represent the official views of the National Institute of Allergy and Infectious Diseases or the National Institutes of Health. The authors would like to thank Dr. Vladimir Dusevich (Director, Electron Microscopy Facility, School of Dentistry, University of Missouri-Kansas City, MO) for the electron microscopy.

REFERENCES

- Poelvoorde N, Verstraelen H, Verhelst R, Saerens B, De Backer E, dos Santos Santiago GL, *et al.* In vivo evaluation of the vaginal distribution and retention of a multi-particulate pellet formulation. *Eur J Pharm Biopharm.* 2009;73(2):280–4.
- Alukda D, Sturgis T, Youan BB. Formulation of tenofovir-loaded functionalized solid lipid nanoparticles intended for HIV prevention. *J Pharm Sci.* 2011;100(8):3345–56.
- Agrahari V, Zhang C, Zhang T, Li W, Gounev TK, Oyler NA, *et al.* Hyaluronidase-sensitive nanoparticle templates for triggered release of HIV/AIDS microbicide *in vitro*. *AAPS J.* 2014;16(2):181–93.
- Meng J, Sturgis TF, Youan BB. Engineering tenofovir loaded chitosan nanoparticles to maximize microbicide mucoadhesion. *Eur J Pharm Sci.* 2011;44(1–2):57–67.
- Meng J, Zhang T, Agrahari V, Ezoulin MJ, Youan BB. Comparative biophysical properties of tenofovir-loaded, thiolated and nonthiolated chitosan nanoparticles intended for HIV prevention. *Nanomedicine.* 2014;9(11):1595–612.
- Zhang T, Zhang C, Agrahari V, Murowchick JB, Oyler NA, Youan BB. Spray drying tenofovir loaded mucoadhesive and pH-sensitive microspheres intended for HIV prevention. *Antivir Res.* 2013;97(3):334–46.
- Bilancetti L, Poncelet D, Loisel C, Mazzitelli S, Nastruzzi C. A statistical approach to optimize the spray drying of starch particles: application to dry powder coating. *AAPS PharmSciTech.* 2010;11(3):1257–67.
- Li X, Anton N, Arpagaus C, Belleteix F, Vandamme TF. Nanoparticles by spray drying using innovative new technology: the Buchi nano spray dryer B-90. *J Control Release.* 2010;147(2):304–10.
- Peltonen L, Valo H, Kolakovic R, Laaksonen T, Hirvonen J. Electrospraying, spray drying and related techniques for production and formulation of drug nanoparticles. *Expert Opin Drug Deliv.* 2010;7(6):705–19.
- Leitner VM, Walker GF, Bernkop-Schnurch A. Thiolated polymers: evidence for the formation of disulphide bonds with mucin glycoproteins. *Eur J Pharm Biopharm.* 2003;56(2):207–14.
- Meng J, Agrahari V, Ezoulin M, Zhang C, Purohit S, Moltenic A, *et al.* Tenofovir containing thiolated chitosan core/shell nanofibers: *in vitro* and *in vivo* evaluations. *Mol Pharmaceutics.* 2016. doi:10.1021/acs.molpharmaceut.6b00739.
- Li X, Kong X, Shi S, Zheng X, Guo G, Wei Y, *et al.* Preparation of alginate coated chitosan microparticles for vaccine delivery. *BMC Biotechnol.* 2008;8:89–100.
- Shinde UA, Nagarsenker MS. Characterization of gelatin-sodium alginate complex coacervation system. *Indian J Pharm Sci.* 2009;71(3):313–7.
- D'Souza SS, DeLuca PP. Development of a dialysis *in vitro* release method for biodegradable microspheres. *AAPS PharmSciTech.* 2005;6(2):E323–8.

15. Sassi AB, Isaacs CE, Moncla BJ, Gupta P, Hillier SL, Rohan LC. Effects of physiological fluids on physical-chemical characteristics and activity of topical vaginal microbicide products. *J Pharm Sci.* 2008;97(8):3123–39.
16. Owen DH, Katz DF. A vaginal fluid simulant. *Contraception.* 1999;59(2):91–5.
17. Zhang Y, Huo M, Zhou J, Zou A, Li W, Yao C, *et al.* DDSolver: an add-in program for modeling and comparison of drug dissolution profiles. *AAPS J.* 2010;12(3):263–71.
18. Han HK, Shin HJ, Ha DH. Improved oral bioavailability of alendronate via the mucoadhesive liposomal delivery system. *Eur J Pharm Sci.* 2012;46(5):500–7.
19. Cardiff RD, Miller CH, Munn RJ. Manual hematoxylin and eosin staining of mouse tissue sections. *Cold Spring Harb Protoc.* 2014;2014(6):655–8.
20. Catalone BJ, Kish-Catalone TM, Budgeon LR, Neely EB, Ferguson M, Krebs FC, *et al.* Mouse model of cervicovaginal toxicity and inflammation for preclinical evaluation of topical vaginal microbicides. *Antimicrob Agents Chemother.* 2004;48(5):1837–47.
21. Bei D, Marszalek J, Youan BB. Formulation of dacarbazine-loaded cubosomes—part I: influence of formulation variables. *AAPS PharmSciTech.* 2009;10(3):1032–9.
22. Singh SK, Banala VT, Gupta GK, Verma A, Shukla R, Pawar VK, *et al.* Development of docetaxel nanocapsules for improving in vitro cytotoxicity and cellular uptake in MCF-7 cells. *Drug Dev Ind Pharm.* 2015;41:1759–68.
23. zur Muhlen A, Schwarz C, Mehnert W. Solid lipid nanoparticles (SLN) for controlled drug delivery—drug release and release mechanism. *Eur J Pharm Biopharm.* 1998;45(2):149–55.
24. Costa P, Sousa Lobo JM. Modeling and comparison of dissolution profiles. *Eur J Pharm Sci.* 2001;13(2):123–33.
25. Aho K, Derryberry D, Peterson T. Model selection for ecologists: the worldviews of AIC and BIC. *Ecology.* 2014;95(3):631–6.
26. Mlisana K, Naicker N, Werner L, Roberts L, van Loggerenberg F, Baxter C, *et al.* Symptomatic vaginal discharge is a poor predictor of sexually transmitted infections and genital tract inflammation in high-risk women in South Africa. *J Infect Dis.* 2012;206(1):6–14.
27. Heng PW, Chan LW, Tang ES. Use of swirling airflow to enhance coating performance of bottom spray fluid bed coaters. *Int J Pharm.* 2006;327(1–2):26–35.
28. Masters K. Spray-air contact, particle formation and drying. Spray drying in practice. Denmark: SprayDryConsult Intl. ApS; 2002. p. 129–191.
29. Maury M, Murphy K, Kumar S, Shi L, Lee G. Effects of process variables on the powder yield of spray-dried trehalose on a laboratory spray-dryer. *Eur J Pharm Biopharm.* 2005;59(3):565–73.
30. Chapter 6. Viscosity. In: Sperling LH, editor. *Introduction to physical polymer science.* 4th ed 2006. p. 77–87.
31. Hamdy S, Haddadi A, Ghotbi Z, Hung RW, Lavasanifar A. Part I: targeted particles for cancer immunotherapy. *Curr Drug Deliv.* 2011;8(3):261–73.
32. Hung RW, Hamdy S, Haddadi A, Ghotbi Z, Lavasanifar A. Part II: targeted particles for imaging of anticancer immune responses. *Curr Drug Deliv.* 2011;8(3):274–81.
33. LeClair DA, Cranston ED, Xing Z, Thompson MR. Optimization of spray drying conditions for yield, particle size and biological activity of thermally stable viral vectors. *Pharm Res.* 2016;33(11):2763–76.
34. Kanojia G, Willems GJ, Frijlink HW, Kersten GF, Soema PC, Amorij JP. A design of experiment approach to predict product and process parameters for a spray dried influenza vaccine. *Int J Pharm.* 2016;511(2):1098–111.
35. Fang Y, Al-Assaf S, Phillips GO, Nishinari K, Funami T, Williams PA, *et al.* Multiple steps and critical behaviors of the binding of calcium to alginate. *J Phys Chem B.* 2007;111(10):2456–62.
36. Lee WA, He GX, Eisenberg E, Cihlar T, Swaminathan S, Mulato A, *et al.* Selective intracellular activation of a novel prodrug of the human immunodeficiency virus reverse transcriptase inhibitor tenofovir leads to preferential distribution and accumulation in lymphatic tissue. *Antimicrob Agents Chemother.* 2005;49(5):1898–906.
37. Chantler E, Debruyne E. Factors regulating the changes in cervical mucus in different hormonal states. *Adv Exp Med Biol.* 1977;89:131–41.
38. Gipson IK, Ho SB, Spurr-Michaud SJ, Tisdale AS, Zhan Q, Torlakovic E, *et al.* Mucin genes expressed by human female reproductive tract epithelia. *Biol Reprod.* 1997;56(4):999–1011.
39. Clift AF. Early studies on the rheology of cervical mucus. *Am J Obstet Gynecol.* 1979;134(7):829–32.
40. Godley MJ. Quantitation of vaginal discharge in healthy volunteers. *Br J Obstet Gynaecol.* 1985;92(7):739–42.
41. Bogataj M, Vovk T, Kerec M, Dimnik A, Grabnar I, Mrhar A. The correlation between zeta potential and mucoadhesion strength on pig vesical mucosa. *Biol Pharm Bull.* 2003;26(5):743–6.